PNAS

Supplementary Information for

Anti-angiogenic properties of microRNA-29a in preclinical ocular models

De-Wei Peng[a,1], Chun-Lin Lan[a,1], Ling-Qin Dong[a], Meng-Xi Jiang[a], Huan Xiao[a], Robert J. D'Amato[c,d], Zai-Long Chi[a,b,*]

*Corresponding author: Zai-Long Chi.
Email: zailong.chi@eye.ac.cn

This PDF file includes:

Supplementary Information Text

Materials and Methods

Corneal micropocket angiogenesis assay

Mice received general anesthesia with an intraperitoneal injection of a mixture of ketamine (85 mg/kg) and xylazine (5 mg/kg). Proparacaine hydrochloride (Alcon, Fort Worth, TX, USA) was used to topically anesthetize the mouse eyes. The intrastromal micropocket was created approximately 1 mm from the limbus in the mouse using the von Graef knife, and then a slow-release pellet containing bFGF was prepared and implanted into the corneal pocket as previously described (1). Mouse corneas implanted with sham pellets without bFGF served as the control group. A subconjunctival injection of agomirs or siRNAs targeting *PDGFC*, *SLC43A2*, or *COL7A1* (2 μg in 10 μl of PBS; RiboBio) was conducted using a 33-gauge needle (Hamilton, Reno, NV, USA) as soon as the model was established. For siRNAs, Entranster reagent (Engreen Biosystem, Auckland, New Zealand) for *in vivo* transfection was used throughout this study according to the manufacturer's instructions. The scrambled agomir (agomir-NC) or negative siRNA (si-NC) was administered as the negative control. Ofloxacin eye ointment was applied to prevent bacterial infection after the surgical procedure. The area of neovascularization was examined under a slit-lamp biomicroscope five days later and quantified using the method described by Birsner et al (2). The mice were euthanized 5 days after pellet implantation, and the corneas without limbus were isolated from the eyeball.

Oxygen-induced retinopathy (OIR)

The OIR model was established as described previously (3-5). Mouse pups with their nursing mother were exposed to 75% oxygen from P7 to P12 and then returned to room air, followed by an intravitreal injection of agomirs or siRNAs complexed with Entranster™ in vivo reagent (Engreen Biosystem) and the corresponding si-NC at a dose of 1 μg dissolved in 1 μl of PBS using a 33-gauge microneedle. At P17, the retinas were isolated from mice with body weights ranging from 5 to 7.5 g for subsequent experiments. The retinas were fixed with 4% paraformaldehyde (PFA) and stained with fluorescent *Griffonia simplicifolia* isolectin B_4 (IB_4; Thermo Fisher Scientific) overnight. Whole-mount retinal images were captured using a confocal microscope (Axio Observer Z1; Carl Zeiss, Oberkochen, Germany). The areas of preretinal tufts (neovascularization) were quantified and analyzed using Adobe Photoshop and ImageJ software. At least three litters of mice from each group were analyzed.

Laser-induced choroidal neovascularization (CNV)

Six-week-old mice were anesthetized by administering an intraperitoneal injection of a mixture of ketamine (85 mg/kg) and xylazine (5 mg/kg). Topical tropicamide (Alcon) was applied to dilate the pupils. Then, laser photocoagulation was induced using an image-guided laser system (Micron IV, Phoenix Research Laboratories, Pleasanton, CA, USA) as previously described by Gong et al. (6). Eyes showing significant subretinal hemorrhage after laser photocoagulation were excluded. Immediately afterward, agomirs or siRNAs (2 μg) or the corresponding si-NC (2 μl in PBS) complexed with Entranster™ in vivo (Engreen Biosystem) were injected intravitreally. The mice were euthanized 7 days after laser photocoagulation, and the anterior segment and neural retina were removed from the eyeball for subsequent experiments. The CNV lesions on choroidal flat mounts were labeled with IB_4 and imaged with an IXplore SpinSR Microscope (Olympus, Tokyo, Japan). The CNV volume (3 dimensions) was calculated and visualized using ImageJ software. The RPE/choroids were isolated from the eyeball (scraped off from the sclera) to detect miR-29 expression levels. Mice without laser photocoagulation were used as the control group.

Quantitative reverse transcription PCR (RT-qPCR)

The corneas (without limbus), neural retina, or RPE/choroid tissues were prepared from CoNV, OIR, or CNV models to analyze RNA expression. Total RNA was extracted from mouse tissues or cultured cells using a Total RNA Kit II (Omega Bio-Tek). RT-qPCR of miRNAs was performed using miDETECT A Track miRNA qRT-PCR Starter Kit and the corresponding primers for miR-29a-3p, miR-29b-3p, or miR-29c-3p (RiboBio). Reverse transcription of mRNAs was performed using the GoScript Reverse Transcription System (Promega, Madison, WI, USA). Real-time PCR

was performed using iTaq Universal SYBR Green Supermix (Bio-Rad, Hercules, CA, USA) and QuantStudio 5 Real-Time PCR Systems (Applied Biosystems, Foster City, CA, USA). U6 small nuclear RNA (snRNA) and *GAPDH* were used as endogenous controls to normalize the expression of miRNAs and mRNAs, respectively. Relative expression levels were determined using the ΔΔCT method (7). All primers used for RT-qPCR are degenerate primers designed based on the conserved regions of human and mouse genes, and their sequences are provided in *SI Appendix*, Table S1.

Cell culture and transfection

HRMECs were obtained from Angio-Proteomie (Peabody, MA, USA). HRMECs were cultured at 37°C with 5% CO_2 in a humidified atmosphere in Endothelial Cell Medium (ECM) containing 5% FBS, 100 μg/ml streptomycin, 100 U/ml penicillin, and 20 μg/ml endothelial cell growth supplement (ECGS). HEK293 cells (ATCC, Manassas, VA, USA) were maintained in high-glucose DMEM (Thermo Fisher Scientific) supplemented with 10% FBS in 5% CO_2 at 37°C. Media were changed every 48 hours. PCR-based mycoplasma detection assays (C0301S, Beyotime) confirmed the lack of mycoplasma contamination in any of the cell lines. Cells were transfected with 50 nM agomirs, antagomirs (chemically modified miRNA inhibitor), or siRNAs and the corresponding NC using Lipofectamine RNAiMAX (Thermo Fisher Scientific) according to the manufacturer's instructions. Table S2 in the *SI Appendix* lists all siRNAs used in this study.

Proliferation assay

HRMECs were seeded in 96-well plates (Costar, USA) at a density of 3×10^3 cells per well and cultured with ECM at 37°C with 5% CO_2 for 24 h. One to 5 days after transfection, cell proliferation was detected using a Cell Counting Kit-8 (Dojindo, Kumamoto, Japan) according to the manufacturer's protocol. The absorbance at 450 nm was read using a Multiscan GO microplate reader (Thermo Fisher Scientific).

Transwell assay

Twenty-four hours after transfection, HRMECs were harvested and resuspended in 0.2 ml of ECM (approximately 1×10^5 cells). The cells were then added to the upper chamber of Transwell inserts with 8-mm pore sizes (Corning, NY) in a 24-well plate. The lower chambers were filled with 0.4 ml of ECM containing 10% FBS and 20 μg/ml ECGS. After 24 h of incubation, the cells that migrated to the underside of the Transwell chambers were fixed with 4% paraformaldehyde for 30 minutes at 4°C and stained with 1% crystal violet (Beyotime Biotechnology, Shanghai, China) for 20 minutes. The images were captured immediately using an inverted microscope (Leica), and the cells were counted using ImageJ software.

Tube formation assay

The cells were plated in 6-well plates and transfected with agomirs, antagomirs, or siRNAs and the corresponding NC when they reached approximately 50% confluence. After 24 hours, the cells were collected and cultured in a 48-well plate (4×10^4 per well), which was precoated with 100 μl of Matrigel Basement Membrane Matrix (BD Biosciences, San Jose, CA, USA). Cells were incubated at 37°C for 6 hours and then imaged with a microscope (Leica) to assess the formation of tube-like structures. The number of meshes and total tube length were quantified using the ImageJ plugin Angiogenesis Analyzer (8).

Scratch wound assay

The HRMECs were plated in 12-well plates (1×10^5 cells per well) and grown to approximately 60% confluence. After transfection, the cells were expanded to 100% confluence. A sterile 200-μl pipette tip was used to create scratches across the confluent cell monolayer. The floating cells and cellular debris were carefully removed by flushing the well with PBS and then replenishing each well with fresh culture medium. Closure of the denuded regions was monitored by capturing images at different time points with the DMi8 inverted microscope.

Histological examination

For the histological analysis, mouse eyes were enucleated and fixed with Methacarn solution for 2 hours. Fixed eyes were dehydrated in increasing alcohol concentrations at room temperature and embedded in paraffin. Sections with a thickness of 4 μm were cut through the optic nerve axis (transverse plane) and stained with hematoxylin and eosin (H&E). Images were collected with an upright BX41 microscope (Olympus, Tokyo, Japan).

Fluorescein angiography (FFA)

Eight-week-old mice were anesthetized by administering an intraperitoneal injection of a mixture of ketamine (85 mg/kg) and xylazine (5 mg/kg). Topical tropicamide (Alcon) was applied to dilate the pupils. Then, the mice were intraperitoneally injected with approximately 0.2 ml of 2% fluorescein sodium (Cardinal Health, Dublin, OH, USA). Digital photographs of the retinal fundus were captured 5 minutes after fluorescein administration using a Micron IV retinal imaging microscope.

Electroretinogram (ERG)

ERGs were recorded with the VEP/ERG System (Model: RETI-port/scan 21, Roland Consult, Germany). Rod and cone functions were assessed by recording scotopic and photopic ERGs, respectively. After 12 hours of dark adaptation, 8-week-old mice were anesthetized as described above. Tropicamide drops (Santen Pharmaceutical Co., Ltd.) were applied to the mouse corneas, and proparacaine drops (Alcon, Canada) were applied for mydriasis and topical corneal anesthesia. Then, the mice were placed onto the heated (37°C) ERG platform. Sodium carboxymethylcellulose was used to lubricate the cornea simultaneously with loop electrode placement. Reference and ground electrodes were placed in the mouth and tail, respectively. Full-field ERGs consisting of the standard specified five responses (rod response, combined rod-cone response, oscillatory potentials, cone response and 30 Hz flicker) proposed by the International Society for the Clinical Electrophysiology of Vision (ISCEV) were recorded (9). ERG waveforms for the a- and b-waves were analyzed using RETI software.

Immunofluorescence staining and immunohistochemistry

Enucleated eyes or whole-mount retinas were fixed with 4% PFA for 30 minutes and rinsed twice with PBS. Eyeball cryosections were prepared in the sagittal plane at a thickness of 12 μm. The sections or retina flat-mounts were incubated in blocking buffer (PBS with 3% BSA, 0.3% Triton X-100) for one hour and stained with IB_4 overnight, followed by a PBS rinse. Then, the sections and retinas were subjected to immunofluorescence staining overnight at 4°C using a primary antibody against GFAP (G3893; Sigma–Aldrich, St. Louis, MO, USA). After three rinses with PBS for 5 minutes each, an Alexa Fluor-488 conjugated secondary antibody (A-11001; Thermo Fisher Scientific) was applied and incubated for 2 hours at room temperature. Finally, the samples were coverslipped with antifade mounting medium containing DAPI (Beyotime) and imaged using a SpinSR confocal microscope (Olympus). For flat-mount retinas, images were further processed with ImarisViewer software (Oxford Instruments, Zurich, Switzerland) to create 3D reconstructions of the retinal vascular network.

Immunohistochemical staining was performed as previously described (10). Sections were stained using a Vector ImmPACT DAB kit (Vector Laboratories, Burlingame, CA, USA). Antibodies against SLC43A2 (D262243) and COL7A1 (D161588) were purchased from Sangon Biotech (Shanghai, China), and the PDGFC antibody (55076-1-AP) was purchased from Proteintech (Rosemont, IL, USA). Images were captured with an upright microscope (BX41; Olympus).

Choroidal sprouting assays

Choroidal sprouting assays were performed as previously described (11). Briefly, the choroid-scleral complex was removed from 4-week-old mice and then cut into approximately 1 × 1 mm pieces. The choroid/sclera fragments without RPE were placed in growth factor-reduced Matrigel (BD Biosciences) seeded in 24-well plates. After the Matrigel was solidified at 37°C (approximately 10 minutes), 500 mL of ECM medium were added to each well and incubated at 37°C for six days. Images were captured with an inverted microscope DMi8 (Leica), and the area of sprouting was analyzed using SWIFT-Choroid macros of ImageJ.

High-throughput sequencing and data analysis

Neural retinal tissues (without RPE/Choroids) were isolated from 8-week-old miR-29a KO and WT littermates. Total RNA was extracted from fresh retinas using a Total RNA Kit II (Omega Bio-Tek). The cDNA libraries were generated using the NEBNext Ultra RNA Library Prep Kit for Illumina (NEB, Ipswich, MA, USA) after removing the ribosomal RNA with the Ribo-Zero kit (Epicenter, Madison, WI, USA) according to the manufacturer's recommendations. The purified library products were evaluated using the Agilent 2200 TapeStation and Qubit 2.0 Fluorometer (Thermo Fisher Scientific). The libraries were sequenced at Novogene Co., Ltd. (Beijing, China) using the Illumina HiSeq 3000 platform. Approximately 60 million reads with a 250-base pair (bp) length were generated. The clean sequencing reads were obtained after removing reads containing adapters or multiple N bases (N refers to any base that the software cannot recognize) and low-quality reads from raw data. HISAT2 (12) was used to align the clean reads to the mouse reference genome mm10 with the default parameters. Differential expression was assessed using DEseq with the FPKM (fragments per kilobase of exon per million fragments mapped) value as the input. Differentially expressed RNAs were chosen according to the criteria of a fold change > 2 and adjusted $P < 0.05$. The Reactome database was adopted to identify significant signaling pathways linked to differentially expressed mRNAs in miR-29a KO mice (13). We chose Fisher's exact test to select significant pathways, and the significance threshold was defined based on its *P* value and FDR. Pathway networks were established by connecting significant signaling pathways and differentially expressed mRNAs to illustrate their biological relationships using Cytoscape software (14). A Gene Ontology (GO) enrichment analysis was performed to clarify the biological functions of the differentially expressed mRNAs using the Cytoscape plug-in ClueGO, which also was used to visualize the nonredundant biological terms for large clusters of genes in a functionally grouped network (15).

Luciferase reporter assays

The 3′UTRs of *SLC43A2*, *COL7A1*, and *PDGFC* were amplified and individually cloned into the pmirGLO vector (Promega) through directional cloning. The mutated seed region was generated using a site-directed mutagenesis method to remove complementary sequences to nucleotides of miR-29a. HEK293 cells were cultured in 96-well plates and cotransfected with 100 ng/well recombinant pmirGLO vector and 50 nM miR-29a or NC with Lipofectamine 2000 Transfection Reagent (Thermo Fisher Scientific). Twenty-four hours after transfection, luciferase activity was detected with a Dual-Glo Luciferase Assay System (Promega) according to the manufacturer's instructions.

Western blot

Total proteins were extracted from mouse corneas, retinas, and RPE/choroid tissues or HRMECs using RIPA lysis buffer (Beyotime Biotechnology), and the concentration was measured using a Pierce BCA Protein Assay Kit (Thermo Fisher Scientific) according to the manufacturer's instructions. Western blot assays were conducted as previously described (16). The PDGFC (55076-1-AP) antibody was purchased from Proteintech. An antibody against PDGFRB was obtained from Abcam (ab69506; Cambridge, MA, USA), and antibodies against ERK (9102L) and phospho-ERK (9101L) were purchased from CST. A GAPDH monoclonal antibody (AF0006) was purchased from Beyotime Biotechnology. Anti-mouse or anti-rabbit immunoglobulin G (IgG) and horseradish peroxidase (HRP)-conjugated antibodies (7076P2 and 7074S, respectively, CST) were used as the secondary antibodies. All antibodies were used according to the manufacturer's instructions. Specific protein bands were detected with Clarity Western ECL Substrate (Bio-Rad, Hercules, CA, USA) and images were captured using a FluorChem E System (ProteinSimple, San Jose, CA, USA). The gray value for the intensity of each protein band was analyzed using ImageJ software.

Statistical analysis

At least three independent experiments were performed for each assay to obtain statistically significant differences. GraphPad Prism software was used for statistical analyses, and the Shapiro-Wilk test was performed on all data to evaluate normality before selecting statistical tests.

Two-tailed Student's *t* test (two groups) or ANOVA followed by the Holm-Sidak or Dunnett's multiple comparison test (more than two groups) were used for the statistical analysis of the data with a normal distribution. The nonparametric Mann-Whitney test (two groups) or Kruskal-Wallis test with linear step-up procedure described by Benjamini, Krieger and Yekutieli for multiple comparisons were used for the statistical evaluation of the data with a skewed distribution. The results are presented as the means ± SEM. A *P* value less than 0.05 was considered significant.

Figures S1 to S6

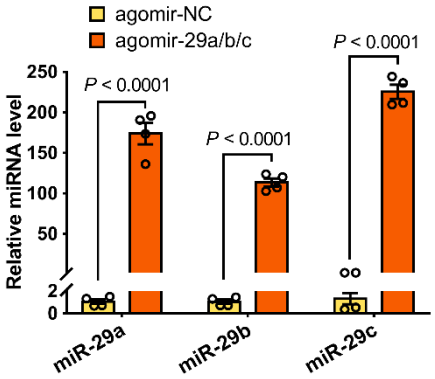

Fig. S1. Relative expression levels of miR-29s in HRMECs after the transfection of agomir-29s. The levels of miR-29s in HRMECs were measured 24 hours after the transfection of agomir-29s using RT-qPCR. Error bars represent the means ± SEM, n = 4 mice per group, Student's t test.

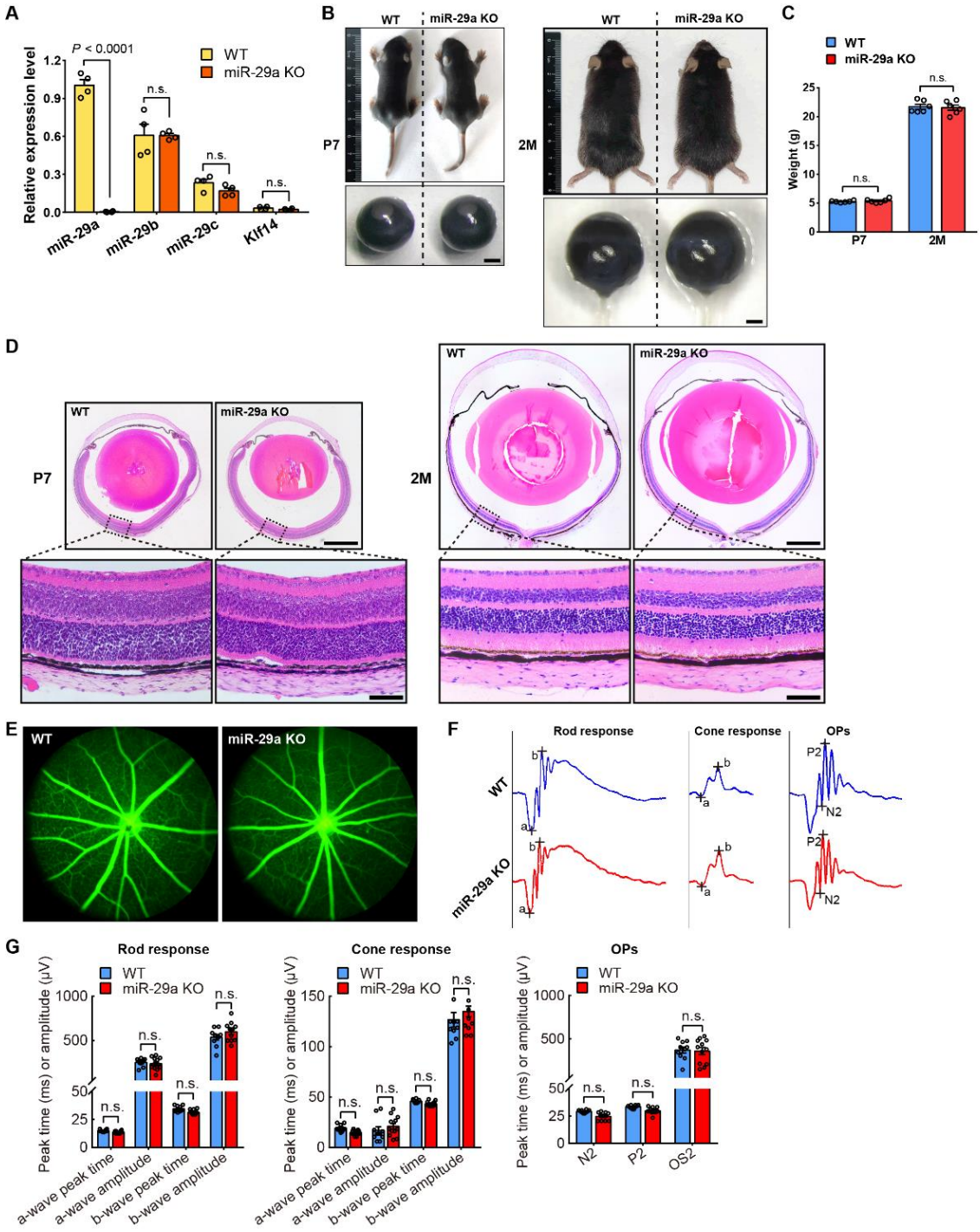

Fig. S2. MiR-29a KO has no adverse effects on the physical and eye development of mouse pups. (*A*) The expression levels of miR-29 family members and the nearby gene Klf14 in miR-29a KO mice and corresponding WT mice (*n* = 4 mice per group). (*B*) Comparisons of body and eyeball size of P7 and adult mice. Scale bars: 500 μm. (*C*) Body weight of pups and adult mice (*n* = 6 mice per group). (*D*) Representative eyeball and retinal sagittal sections from WT and miR-29a KO mice at preweaning (P7, left panel) and postweaning (8 weeks old, right panel) ages. Scale bars: 500 μm; magnified images: 50 μm. (*E*) Representative FFA images (two minutes after dye injection) of 2-month-old miR-29a KO and WT mice. (*F*) Typical ERGs of miR-29a KO and WT mice. (*G*) Wave peak time or amplitude in scotopic and photopic ERGs of miR-29a KO or WT

mice. OPs: oscillatory potentials. *n* = 10-12. Data are presented as the means ± SEM and were analyzed using two-tailed Student's *t* test.

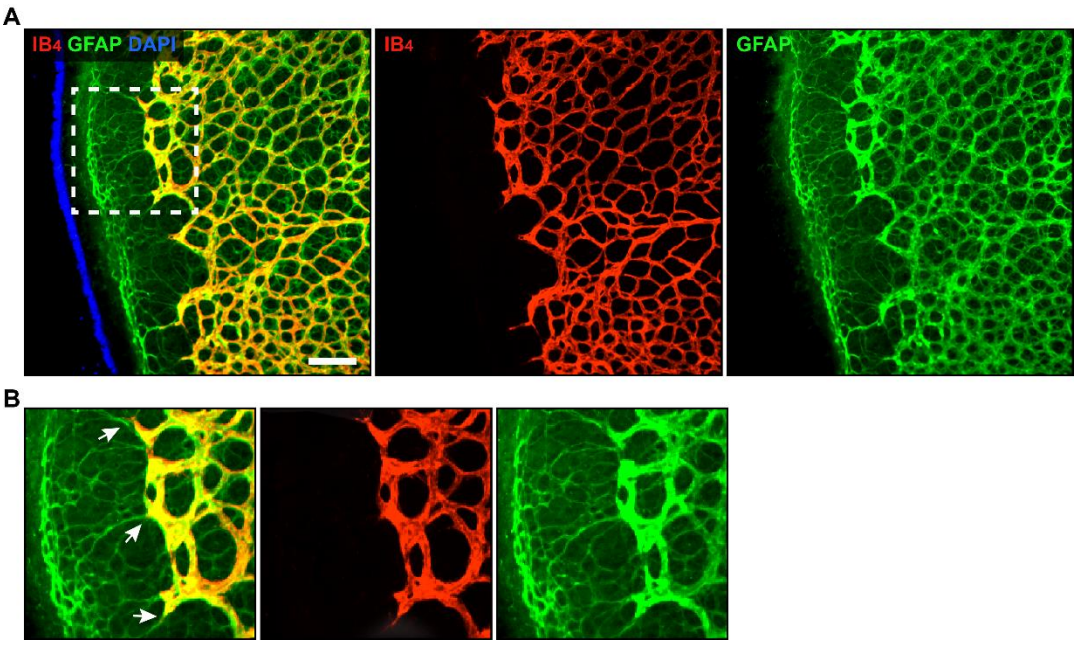

Fig. S3. The vascular tree expands along the astrocyte template during retinal superficial vascular plexus development. (*A*) Representative images of the retina stained with IB_4 (red) and GFAP (green) and counterstained with DAPI (blue). (*B*) Higher magnification images are displayed. White arrows in magnified images show the vascular branches following the "path" of astrocytes. Scale bars: 200 μm.

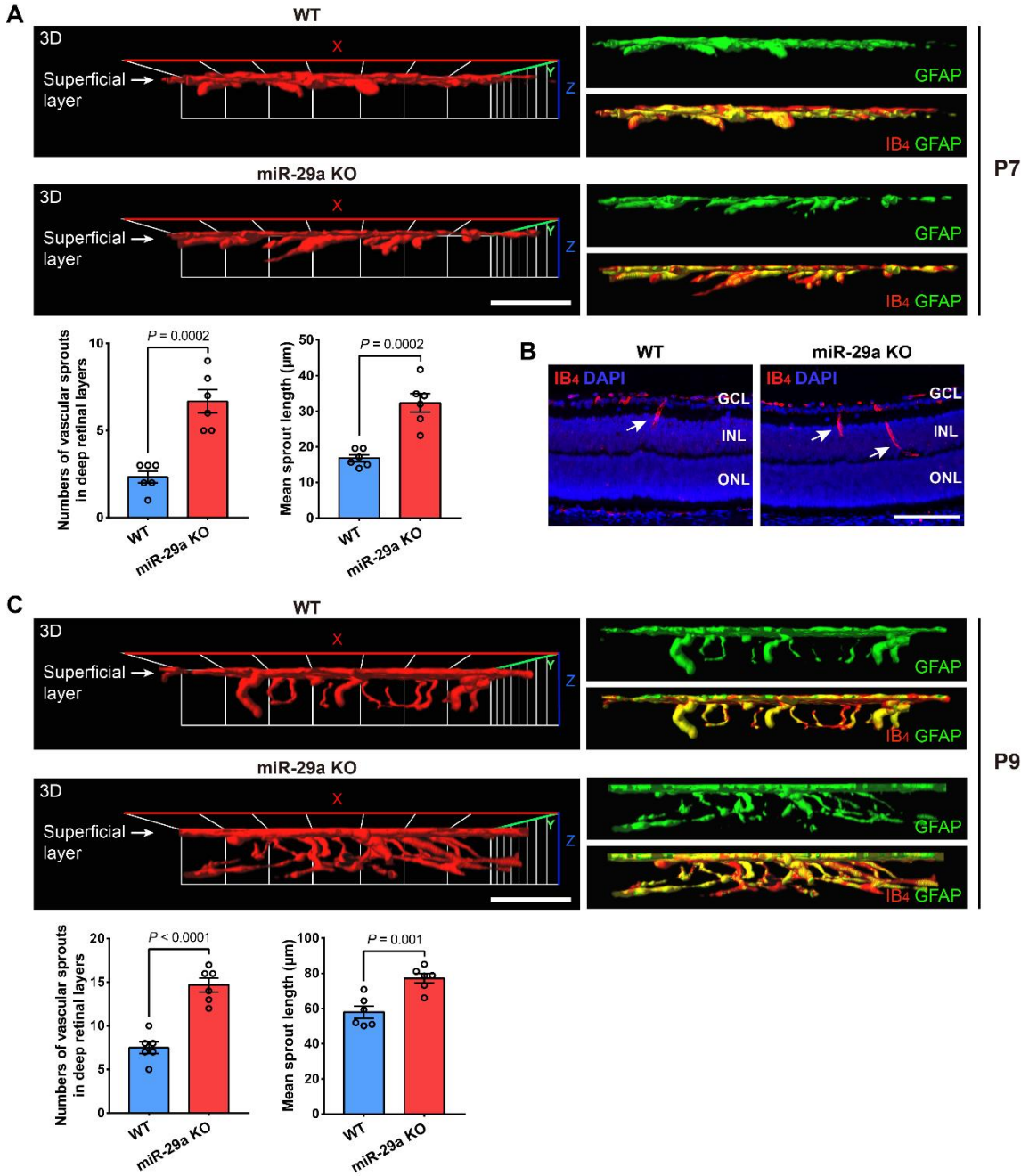

Fig. S4. Knockout of miR-29a accelerates vessel sprouting into the deeper retinal layers. (*A* and *C*) Three-dimensional (3D) reconstruction of retinal vasculature networks showing vertical sprouts originating from the superficial plexus at P7 (*A*) and P9 (*C*) and quantification of the sprout numbers and length (n = 6 mice per group). The retinas were immunostained with IB_4 and a GFAP antibody. (*B*) Representative confocal images of retinal sagittal sections at P7 stained for IB_4. Nuclei were counterstained with DAPI. GCL, ganglion cell layer; INL, inner nuclear layer; ONL, outer nuclear layer. Error bars indicate SEM; n.s., not significant; Student's *t* tests. Scale bars: 100 μm.

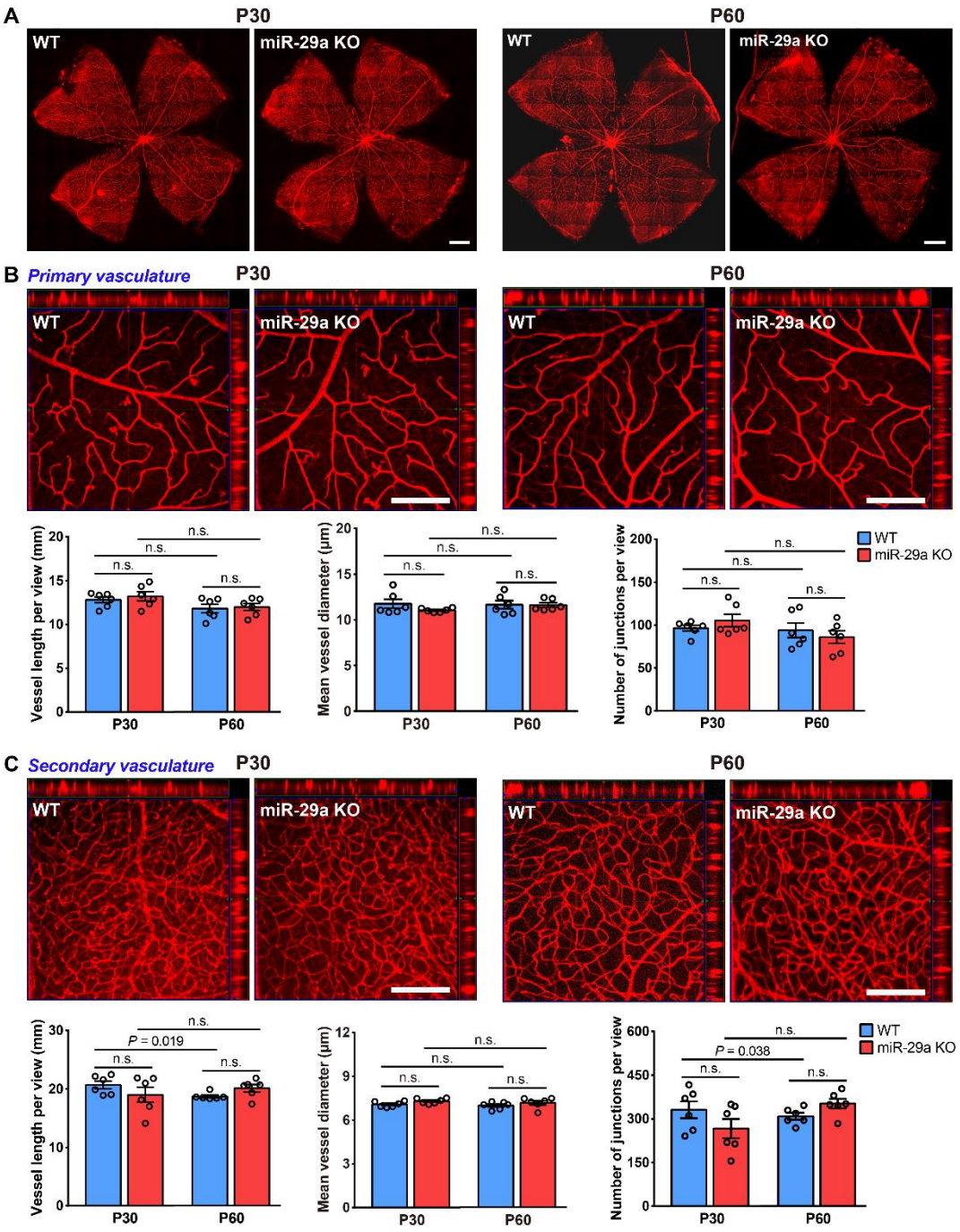

Fig. S5. MiR-29a deletion does not affect the final maturation and stabilization of the 3D retinal vasculature. (*A*) IB_4 staining of whole-mount retinas from P30 and P60 (adult) mice. (*B*) Confocal micrographs (orthogonal view) of the IB_4-labeled retinal primary vasculature and quantification of vessel length, diameter, and junction number. (*C*) Representative images of the retinal secondary vasculature and comparison of vessel length, diameter, and junction number. Error bars represent the means ± SEM (n = 6), using Student's t test; n.s., not significant. Scale bars: 500 μm (*A*) and 200 μm (*B* and *C*).

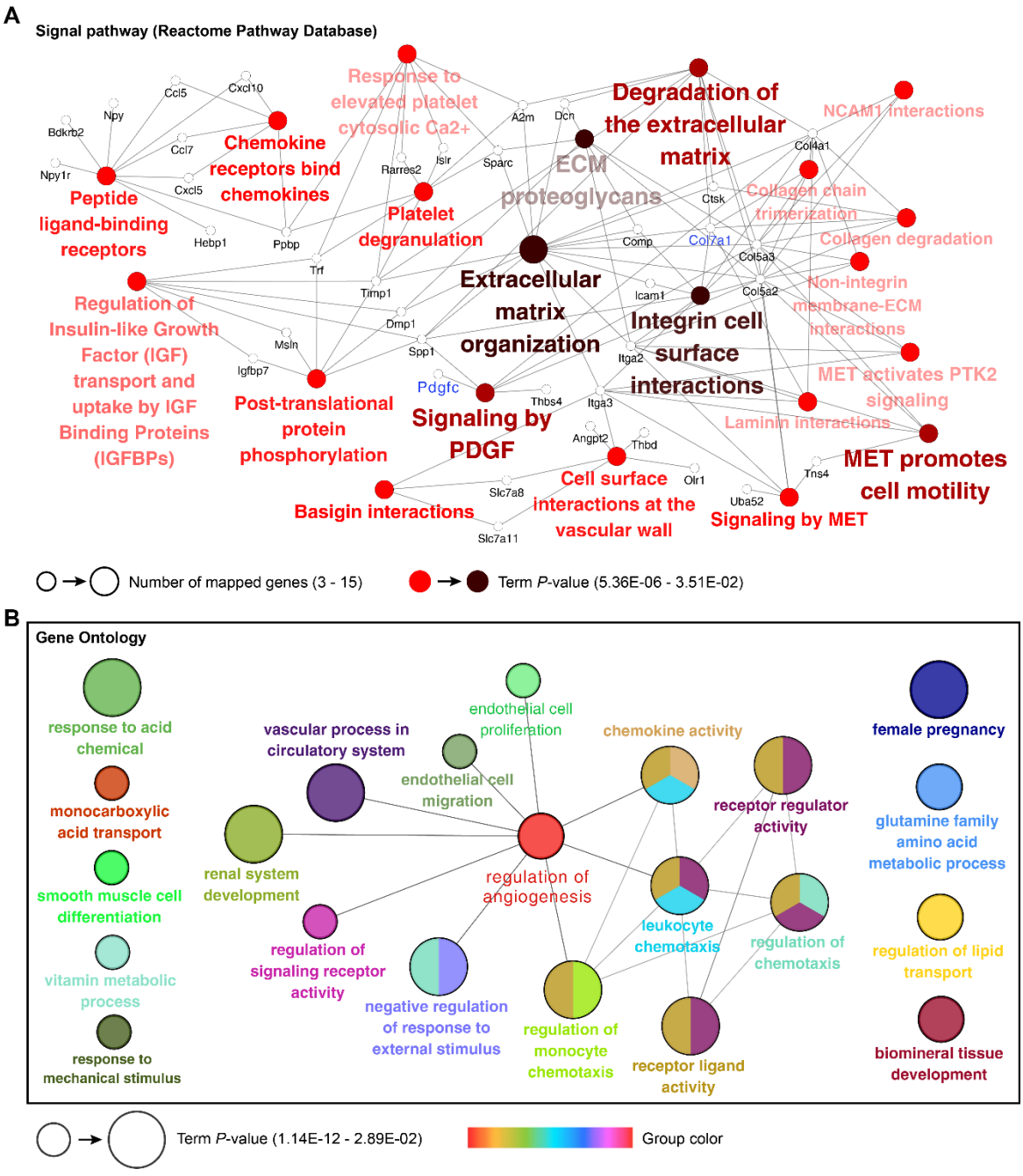

Fig. S6. Signaling pathway and GO analysis of miR-29a KO mice. (*A*) Significant signaling pathways modulated by miR-29a. (*B*) The GO enrichment analysis indicates that miR-29a regulates multiple angiogenesis-related biological processes, including angiogenesis and chemokine activity.

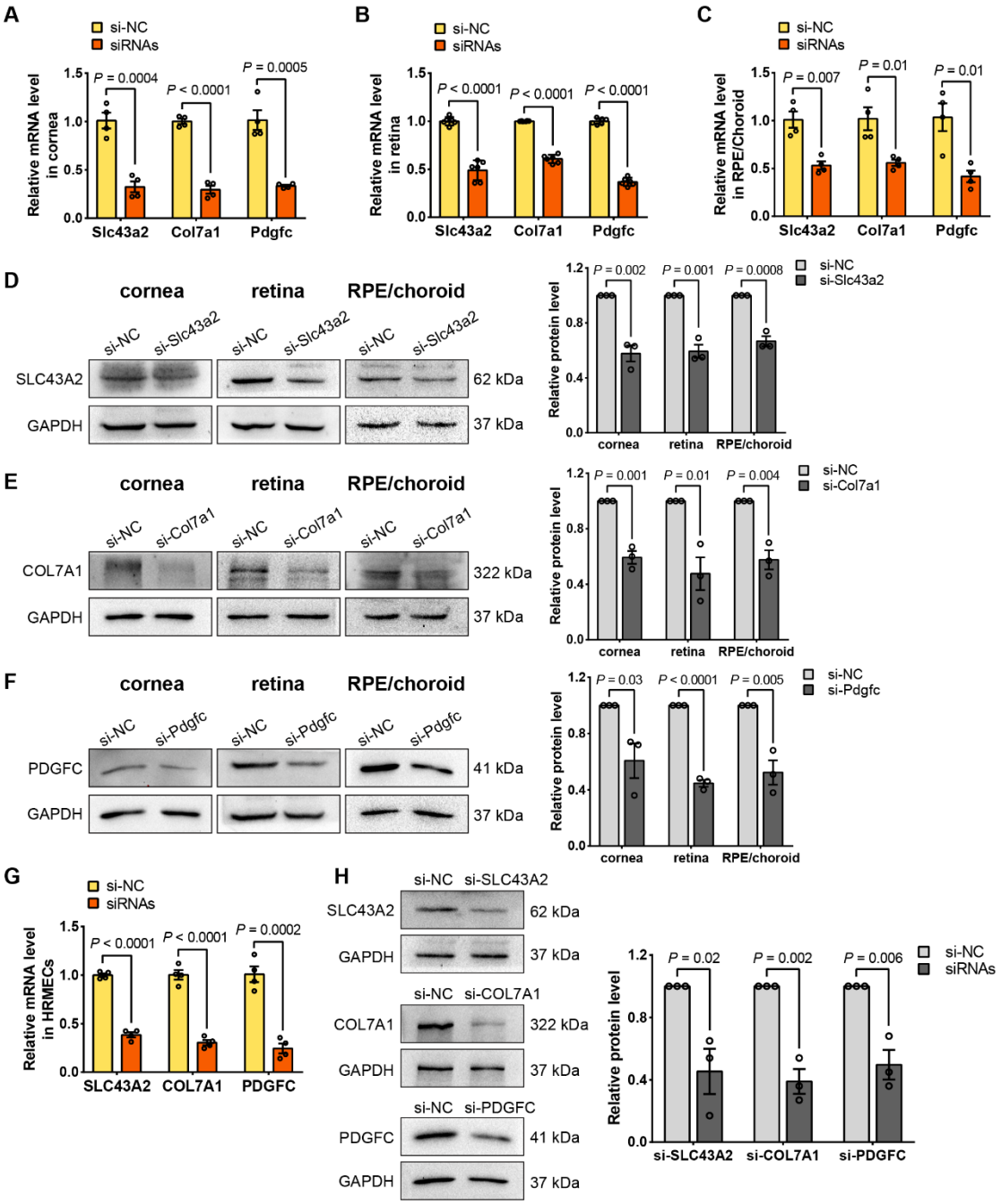

Fig. S7. The knockdown efficiency of siRNAs targeting *Slc43a2*, *Col7a1* or *Pdgfc in vivo* and *in vitro*. (*A-C*) The mRNA levels of miR-29a target genes in cornea (*A*), retina (*B*), or RPE/choroid (*C*) tissues 3 days after the subconjunctival or intravitreal injection of the related siRNAs were determined using RT-qPCR (n = 4-6). si-NC, negative control of siRNA. (*D-F*) The protein levels of miR-29a target genes in the cornea, retina, or RPE/choroid 3 days after the subconjunctival or intravitreal injection of si-Slc43a2 (*D*), si-Col7a1 (*E*), or si-Pdgfc (*F*), as detected using Western blot assays (n = 3). (*G*) The relative mRNA levels of *SLC43A2*, *COL7A1* and *PDGFC* in HRMECs at 24 hours after transfection with the corresponding siRNAs (n = 4). (*H*) The relative protein levels of SLC43A2, COL7A1 and PDGFC in HRMECs at 48 hours after the transfection of the corresponding siRNAs (n = 3). Data are presented as the means ± SEM and were analyzed using two-tailed Student's *t* test.

Tables S1 and S2

Table S1. Sequence of primers used in the RT-qPCR.

Gene Name	Forward Primer (5′→3′) *	Reverse Primer (5′→3′)
COL4A1	CCGCCCTTCTGCTCCACGA	GCCCCTCAGGTCCTTGCAT
COL5A2	TGAAGAAATAGCCTGYACTCA	TCYKGGCAYTCTATCTTGTCAC
SPARC	GCAGCAATGACAACAAGACCT	ATTCRGTCAGCTCRGARTCCA
SLC43A2	CGGTCCACRTTTATTGCCTT	TGATCTTCACCGAGTAGTCCA
COL7A1	ATGARRCACCRGATACTCCC	CTCKCGGTCYCCRACAAG
PDGFC	GCCTGTTGTCTCCAYAATTGC	ACACAGTCACAYTCCTCRT
Klf14	GATTACGCCCGCATCCAAGC	AACTTCTTGTCGCAGTCGAG

* R = G/A, Y = C/T, K = G/T, W = A/T, S = C/G, M = A/C in the sequences

Table S2. List of siRNAs.

Target *	**siRNA Name**	**Antisense Sequence (5′→3′)**
SLC43A2 (hsa or mmu)	si-SLC43A2-1	CCGCCCTTCTGCTCCACGA
	si-SLC43A2-2	CUGAACUUGAUCUUCACCGAG
	si-SLC43A2-3	UGAUCUUGUGGUCAAAGCCUA
COL7A1 (hsa)	si-COL7A1-1	UAAGAACACAAUGUCAGCGGC
	si-COL7A1-2	UCUCGUGGAGCAGAGGUCGAG
	si-COL7A1-3	UGUACUGGACCUUGUAGCCAG
CoL7A1 (mmu)	si-Col7a1-1	UUCUUGUUGCAUCUGAUGCGA
	si-Col7a1-2	UGUCUGUGGAUCAUCACUGUA
	si-Col7a1-3	AAGAAGAAGAAAUCGCUGGUU
PDGFC (has or mmu)	si-PDGFC-1	UCAGAUACAAAUCUUAUCCUG
	si-PDGFC-2	UCUACAAAAUCAUACUUGCAU
	si-PDGFC-3	AAGAAGAAGAAAUCGCUGGUU
Negative control (hsa or mmu)	si-NC	UUCUCCGAACGUGUCACGU

* hsa, Homo sapiens; mmu, Mus musculus

SI References

1. Rogers MS, Birsner AE, & D'Amato RJ (2007) The mouse cornea micropocket angiogenesis assay. *Nat Protoc* 2(10):2545-2550.
2. Birsner AE, Benny O, & D'Amato RJ (2014) The corneal micropocket assay: a model of angiogenesis in the mouse eye. *J Vis Exp* (90).
3. Smith LE*, et al.* (1994) Oxygen-induced retinopathy in the mouse. *Invest Ophthalmol Vis Sci* 35(1):101-111.
4. Connor KM*, et al.* (2009) Quantification of oxygen-induced retinopathy in the mouse: a model of vessel loss, vessel regrowth and pathological angiogenesis. *Nat Protoc* 4(11):1565-1573.
5. Stahl A*, et al.* (2010) Postnatal weight gain modifies severity and functional outcome of oxygen-induced proliferative retinopathy. *Am J Pathol* 177(6):2715-2723.
6. Gong Y*, et al.* (2015) Optimization of an Image-Guided Laser-Induced Choroidal Neovascularization Model in Mice. *PLoS One* 10(7):e0132643.
7. Livak KJ & Schmittgen TD (2001) Analysis of relative gene expression data using real-time quantitative PCR and the 2(-Delta Delta C(T)) Method. *Methods* 25(4):402-408.
8. Carpentier G*, et al.* (2020) Angiogenesis Analyzer for ImageJ - A comparative morphometric analysis of "Endothelial Tube Formation Assay" and "Fibrin Bead Assay". *Sci Rep* 10(1):11568.
9. McCulloch DL*, et al.* (2015) ISCEV Standard for full-field clinical electroretinography (2015 update). *Doc Ophthalmol* 130(1):1-12.
10. Shi SR, Liu C, & Taylor CR (2007) Standardization of immunohistochemistry for formalin-fixed, paraffin-embedded tissue sections based on the antigen-retrieval technique: from experiments to hypothesis. *J Histochem Cytochem* 55(2):105-109.
11. Shao Z*, et al.* (2013) Choroid sprouting assay: an ex vivo model of microvascular angiogenesis. *PLoS One* 8(7):e69552.
12. Kim D, Langmead B, & Salzberg SL (2015) HISAT: a fast spliced aligner with low memory requirements. *Nat Methods* 12(4):357-360.
13. Jassal B*, et al.* (2020) The reactome pathway knowledgebase. *Nucleic Acids Res* 48(D1):D498-D503.
14. Shannon P*, et al.* (2003) Cytoscape: a software environment for integrated models of biomolecular interaction networks. *Genome Res* 13(11):2498-2504.
15. Bindea G*, et al.* (2009) ClueGO: a Cytoscape plug-in to decipher functionally grouped gene ontology and pathway annotation networks. *Bioinformatics* 25(8):1091-1093.
16. Guan JT*, et al.* (2020) MicroRNA-18a-5p Administration Suppresses Retinal Neovascularization by Targeting FGF1 and HIF1A. *Front Pharmacol* 11:276.